Receptor-Mediated Changes at the Myristoylated Amino Terminus of $G\alpha_{il}$ Proteins[†]

Anita M. Preininger, Joseph Parello, Scott M. Meier, Guihua Liao, and Heidi E. Hamm*

Department of Pharmacology, Vanderbilt University Medical Center, Nashville, Tennessee 37232-6600

Received April 25, 2008; Revised Manuscript Received July 8, 2008

ABSTRACT: G protein-coupled receptors (GPCRs) catalyze nucleotide release in heterotrimeric G proteins, the slow step in G protein activation. $G_{i/o}$ family proteins are permanently, cotranslationally myristoylated at the extreme amino terminus. While myristoylation of the amino terminus has long been known to aid in anchoring G_i proteins to the membrane, the role of myristoylation with regard to interaction with activated receptors is not known. Previous studies have characterized activation-dependent changes in the amino terminus of Gα proteins in solution [Medkova, M. (2002) *Biochemistry 41*, 9963−9972; Preininger, A. M. (2003) *Biochemistry 42*, 7931−7941], but changes in the environment of specific residues within the $G\alpha_{i1}$ amino terminus during receptor-mediated G_i activation have not been reported. Using site-specific fluorescence labeling of individual residues along a stretch of the $G\alpha_{il}$ amino terminus, we found specific changes in the environment of these residues upon interaction with the activated receptor and following GTPγS binding. These changes map to a distinct surface of the amino-terminal helix opposite the Gβγ binding interface. The receptor-dependent fluorescence changes are consistent with a myristoylated amino terminus in the proximity of the membrane and/or receptor. Myristoylation affects both the rate and intensity of receptor activation-dependent changes detected at several residues along the amino terminus (with no significant effect on the rate of receptor-mediated GTPγS binding). This work demonstrates that the myristoylated amino terminus of $G\alpha_{il}$ proteins undergoes receptor-mediated changes during the dynamic process of G protein signaling.

GPCRs[1] act as GEFs for heterotrimeric G proteins, catalyzing nucleotide exchange on Gα subunits, which is the rate-limiting step in G protein activation. Agonist-mediated activation of GPCRs is coupled to GDP release by a mechanism which can be probed using biophysical techniques. While crystal structures for a number of G proteins and their respective subunits (*1*−*7*), as well as those of the prototypical GPCR, rhodopsin (*8, 9*), and more recently the β2-adrenergic receptor (*10*), reveal much of what we know about the structure and function of these proteins, there is currently no high-resolution structure of an activated receptor in complex with its cognate G protein. Thus, biophysical and biochemical studies provide valuable insights into the structural determinants and dynamics of G protein activation. A functional heterotrimer is known to be essential for receptor-mediated G protein activation; the amino-terminal region of Gα directly participates in heterotrimer formation, facilitating high-affinity Gα−βγ binding (*11, 12*).

The amino terminus of Gα [as well as the C-terminus (*13, 14*) and α4−β6 loop (*15*)] has been implicated in receptor-mediated interactions in a number of biochemical studies. One of the first reports of such an interaction arose from the observation that a 15-residue peptide encompassing amino-terminal residues 8−23 of $G\alpha_t$ competitively inhibited rhodopsin−G_t interaction but alone did not stabilize metarhodopsin II formation (*16*). More recently, activated rhodopsin was found to cross-link to residues 19−28 spanning the amino-terminal region of native $G\alpha_t$ (*17*). The amino terminus of $G\alpha_q$ has also been implicated in the selectivity of receptor coupling, as addition of amino-terminal $G\alpha_q$-specific residues to the amino terminus of $G\alpha_{i/o}$ proteins conferred the ability of this chimera to couple to G_q-coupled receptors, as measured by phosphatidylinositol hydrolysis (*18*). These studies indicate a specific interaction between the amino terminus of Gα proteins and activated receptors.

$G\alpha_{i/o}$ family members (including $G\alpha_t$) are permanently, cotranslationally modified by myristate (consisting of 14 carbons) at the amino-terminal glycine residue, increasing the hydrophobicity of this region. Myristoylation enhances Gα−βγ subunit association (*19*), but it is not essential for this association. In vitro, myristoylation of Gα and farnesylation of the γ subunit of Gβγ are functionally redundant in facilitating coupling to activated receptors (*20*), as the

[†] This work supported by NIH Grant EY06062.

* To whom correspondence should be addressed: Department of Pharmacology, Vanderbilt University Medical School, 23rd Ave. South at Pierce, Nashville, TN 37232. Phone: (615) 343-3533. Fax: (615) 343-1084. E-mail: heidi.hamm@vanderbilt.edu.

[1] Abbreviations: GPCR, G protein-coupled receptor; G protein, $G\alpha_i\beta_1\gamma_1$ heterotrimer; GEF, guanine nucleotide exchange factor; N-terminus, amino terminus; Hexa I, $G\alpha_{il}$ isoform lacking six solvent-exposed cysteines; GDP, guanosine diphosphate; GTP, guanosine triphosphate; GTPγS, guanosine 5′-*O*-(3-thiotriphosphate); G_t, G protein of the rod outer segment, transducin; G_i, family of G proteins coupled to inhibition of adenylyl cyclase; Gα, α subunits of G proteins; EPR, electron paramagnetic resonance; Gβγ, $G\beta_1\gamma_1$ subunit derived from native G_t; ROS, membranes from rod outer segments containing rhodopsin; SDS, sodium dodecyl sulfate; PMSF, phenylmethanesulfonyl fluoride; A1, Alexa; BD, Bodipy; DTT, dithiothreitol; NMT, *N*-myristoyltransferase; MES, 2-(*N*-morpholino)ethanesulfonic acid; Tris, tris(hydroxymethyl)aminomethane; FRET, fluorescence resonance energy transfer; MI, metarhodopsin I; MII, metarhodopsin II; MIII, metarhodopsin III; AU, arbitrary units; sem, standard error of the mean; ex, excitation; em, emission; em_{max}, emission maximum.

10.1021/bi800741r CCC: $40.75
Published on Web 09/05/2008

ability of an unmyristoylated Gα protein (in complex with Gβγ) to undergo receptor-mediated GTPγS binding was dependent on farnesylation of the Gγ subunit. A recent study of the functional significance of myristoylation which was conducted in transgenic mice revealed a role for myristoylation in deactivation of $G\alpha_t$ subunits. In mice expressing a myristoylation deficient form of $G\alpha_t$, the fraction of unmyristoylated proteins properly localized to rod outer segments (ROS) was found to be activation competent, with the remainder of $G\alpha_t$ mislocalized to inner compartments (*21*). The properly localized (unmyristoylated) $G\alpha_t$ fraction in the ROS was able to bind Gβγ and undergo receptor-mediated GTPγS binding similar to native $G\alpha_t$ but had defects in deactivational processes such as GTPase activity and PDE-mediated GAP activity (*21*). These data point to a role for myristoylation beyond that of simple membrane localization and Gβγ binding.

Using biochemical and biophysical studies of purified, fluorescently labeled myristoylated (and unmyristoylated $G\alpha_{il}$ proteins) and membrane-bound receptors, we demonstrate here that specific amino-terminal residues of $G\alpha_{il}$ proteins undergo receptor-mediated changes during the dynamic process of G protein activation. To examine changes at individual positions along the amino terminus, residues of interest in the amino terminus of a $G\alpha_{il}$ protein lacking solvent-exposed cysteines ($G\alpha_{il}$ Hexa I) were mutated to cysteine, followed by thiol-directed fluorescence labeling. The receptor-mediated environmental changes in individual amino-terminal $G\alpha_{il}$ residues reported here, and the effect of myristoylation on those changes, together shed light on receptor-mediated changes that are communicated through the amino terminus of $G\alpha_{il}$ proteins.

MATERIALS AND METHODS

Materials. GDP and GTPγS were purchased from Sigma-Aldrich (Milwaukee, WI). BODIPY 630 methyl bromide [8-bromomethyl-4,4-difluoro-3,5-bis(2-thienyl)-4-bora-3a,4a-diaza-*s*-indacene, MW 449 (BD^{630})] and Alexa Fluor 594 C_5-maleimide (A1) were purchased from Invitrogen (Madison, WI). All other reagents and chemicals were of the highest available purity.

Preparation of Fluorescently Labeled G Proteins. To examine changes in specific residues using thiol-directed labels, we used a parent $G\alpha_{il}$ in which solvent-exposed cysteines were conservatively replaced via site-directed mutagenesis, and then this construct was used as a basis for site-specific cysteine mutagenesis within the amino terminus. Construction, expression, purification, and fluorescent labeling of $G\alpha_{il}$ and $G\alpha_{il}$ Hexa I proteins (unmyristoylated and myristoylated) were performed as described previously (*22, 23*), with minor modifications. Briefly, the parent $G\alpha_{il}$ Hexa I lacking solvent-exposed cysteines was generated with an expression vector encoding rat $G\alpha_{i1}$ with six amino acid substitutions at solvent-exposed cysteines (C3S/C66A/C214S/C305S/C325A/C351I) and a hexahistidine tag between amino acid residues M119 and T120. This construct served as the template for the introduction of individual cysteine substitutions at sites of interest using the QuickChange system (Stratagene, La Jolla, CA) as previously described; DNA sequencing confirmed all mutations. The mutant constructs are termed $G\alpha_{il}$ Hexa I, followed by the site of cysteine substitution and followed by M if the protein is expressed as a myristoylated protein. For example, Hexa I-13CM refers to the $G\alpha_{il}$ Hexa I parent protein containing a cysteine substitution at the 13th residue and expressed with *N*-myristoyltransferase to yield myristoylated protein, whereas Hexa I-13C is the same protein expressed in the absence of the *N*-myristoyltransferase vector to produce the unmyristoylated counterpart. The mutant constructs were expressed in *Escherichia coli* BL21-Gold (DE3) with or without an *N*-myristoyltransferase (NMT) vector pbb131, which also encodes kanamycin resistance for selection of myristoylated proteins (generously provided by M. Linder, Washington University, St. Louis, MO), and purified as detailed previously (*23*). Coomassie staining of urea SDS−PAGE gels (*24*) demonstrates $G\alpha_{il}$ Hexa I proteins are fully myristoylated (*23*) when coexpressed with the NMT vector. Purified proteins were stored at −80 °C in buffer A containing 50 mM Tris, 100 mM NaCl, 2 mM $MgCl_2$, 10 μM GDP (pH 7.5), and 10% (v/v) glycerol; wild-type $G\alpha_{il}$ containing native, solvent-exposed cysteines was additionally supplemented with 5 mM β-mercaptoethanol or 1 mM DTT prior to being stored at −80 °C. After purification, all proteins used in this study were greater than 85% pure, as estimated by Coomassie staining of SDS−polyacrylamide gels.

$G\alpha_{il}$ Hexa I proteins were labeled as described previously (*22, 23*) using the A1 probe (Invitrogen) with a labeling time of 1 h. Extensive washing with buffer A in a 10 kDa molecular mass concentrator separated labeled protein from unbound probe, followed by spin column and gel filtration purification of labeled proteins, resulting in a labeling efficiency between 0.25 and 0.6 mol of label/mol of protein for all A1-labeled Hexa I proteins (measured by comparing label to protein concentration, $\varepsilon_{588} = 96000\ cm^{-1}\ M^{-1}$ for the A1 probe and protein concentrations as determined by the Bradford assay). All labeled $G\alpha_{il}$ Hexa I proteins used in these assays demonstrated a ≥40% increase in intrinsic tryptophan emission upon AlF_4^- activation after labeling, as expected for properly folded and functional Gα proteins (*25*). This is consistent with previous results demonstrating amino-terminally labeled $G\alpha_{il}$ Hexa I proteins are activation competent and retain the ability to bind to $G\beta_1\gamma_1$ (*22, 23*). $G\beta_1\gamma_1$ (native, bovine, containing multiple solvent-exposed cysteines) was labeled as described above with the thiol-reactive probe BD^{630} (Invitrogen), resulting in a labeling efficiency of >0.85 mol of label/mol of protein, using an ε_{635} of $73000\ cm^{-1}\ M^{-1}$.

Preparation of ROS, Detergent-Solubilized Rhodopsin, and $G\beta_1\gamma_1$. Urea-washed rod outer segment (ROS) membranes containing dark-adapted rhodopsin were prepared as previously described (*26*) and stored protected from light at −80 °C in a buffer containing 10 mM MOPS, 200 mM NaCl, 2 mM $MgCl_2$, 1 mM dithiothreitol (DTT), and 100 μM phenylmethanesulfonyl fluoride (PMSF). ROS detergent solubilization for supplementary experiments was performed as follows (*42*). Under dim red light, urea-washed dark-adpated ROS membranes were solubilized in 50 mM Tris (pH 7.5) containing 100 mM NaCl and dodecyl maltoside (DM) to a final concentration of 0.5% at 4 °C with gentle agitation for 15 min. Insoluble material was removed by centrifugation at 20000*g* for 1 h at 4 °C, and the concentration of solubilized rhodopsin in the supernatant was determined using an ε_{500} of $40600\ cm^{-1}\ M^{-1}$. DM-solubilized

dark rhodopsin thus obtained was substituted for ROS membranes in the assay of receptor-mediated fluorescence intensity changes upon light activation in labeled proteins as described below. These supplementary assays (conducted with soluble receptors) employed a final concentration of 750 nM DM-solubilized rhodopsin, 0.01% DM, and 200 nM A1-labeled $G\alpha_{il}$ Hexa I protein in complex with $G\beta_1\gamma_1$ in assay buffer, to determine the ability of solubilized rhodopsin to mediate light-dependent changes in emission from amino-terminally labeled $G\alpha_{il}$ Hexa I proteins in complex with native $G\beta_1\gamma_1$. $G\beta_1\gamma_1$ (hereafter termed $G\beta\gamma$) was purified from bovine retina as described previously (*26*) and stored in a buffer containing 10 mM Tris, 100 mM NaCl, 5 mM β-mercaptoethanol (BME) (pH 7.5), and 10% (v/v) glycerol.

Intrinsic Tryptophan Fluorescence. To monitor the ability of $G\alpha_{il}$ Hexa I proteins to undergo activation, both before and after labeling, intrinsic tryptophan (Trp^{207} in $G\alpha_t$, analagous to Trp^{211} in $G\alpha_i$) fluorescence was measured as previously described (*25*). Briefly, labeled proteins (100 nM) in buffer A [50 mM Tris, 100 mM NaCl, and 1 mM $MgCl_2$ (pH 7.5)] containing 10 μM GDP were monitored by excitation at 280 nm and emission at 340 nm before and after the addition of AlF_4^- (10 mM NaF and 50 μM $AlCl_3$) using a Varian Cary Eclipse spectrofluorometer. Properly folded and functional $G\alpha$ subunits demonstrate a $\geq$40% increase in intrinsic tryptophan emission upon AlF_4^- activation, in comparison to emission in the basal, GDP-bound state (*25*).

Binding of Labeled $G\alpha_{il}$ Hexa I Proteins to $G\beta\gamma$. Subunit binding was assessed in buffer A (supplemented with 10 μM GDP) using increasing amounts of $G\beta\gamma$ and 10 nM A1-labeled unmyristoylated $G\alpha_{il}$ Hexa I-3C [as previously described for fluorescently labeled Hexa I proteins (*22*)], with excitation (ex) and emission (em) at 570 and 616 nm, respectively. Changes in maximal emission (compared to basal emission in the absence of $G\beta\gamma$) were plotted as a function of increasing $G\beta\gamma$ concentration and fitted using a sigmoidal dose−response curve using Prism 4.0 (Graphpad Software). For myristoylated proteins, the binding affinity was determined by FRET between labeled subunits (*23*), which are relatively solvent-protected and immobile even in the absence of $G\beta\gamma$ proteins (*23*), preventing efficient detection of binding by the relatively simpler protocol used for unmyristoylated proteins. Binding between A1-labeled myristoylated $G\alpha_{il}$ Hexa I-3CM (10 nM) and increasing amounts of $G\beta\gamma$-BD^{630} in buffer A was assessed as a decrease in donor emission as a result of FRET, with ex and em at 570 and 612 nm, respectively, less emission changes in the absence of labeled $G\alpha$ subunits, and fitted to a sigmoidal dose−response curve with Prism 4.0 (GraphPad Software).

Receptor-Mediated Fluorescence Intensity Changes in Labeled Proteins. Labeled $G\alpha_{il}$ Hexa I proteins were reconstituted with $G\beta\gamma$ at 4 °C prior to addition of excess dark ROS, which was then transferred to a cuvette containing buffer A, with final concentrations of 400 nM $G\alpha$ protein, 800 nM $G\beta\gamma$, and 2 μM rhodopsin. All manipulations involving dark rhodopsin were performed in the dark or under dim red light to prevent its activation. The emission (dark spectra) from the cuvette containing dark ROS and A1-labeled subunits in complex with $G\beta\gamma$ was scanned between 580 and 750 nm (5 nm bandpass) with excitation at 575 nm (2.5 nm bandpass) at 21 °C using a Varian Cary Eclipse instrument. After the dark spectrum had been collected, cuvettes were subjected to light activation, and light spectra were collected in duplicate 4 min after the photoactivation of rhodopsin by a Vivitar electronic flash assembly. Finally, GTPγS spectra were collected in duplicate 4 min after the addition of GTPγS (40 μM) to the light-activated sample in the cuvette. While duplicate readings were averaged for the light and GTPγS spectra, the dark spectrum was collected only once prior to light activation to prevent spurious activation of rhodopsin.

Time-Dependent Changes in Fluorescently Labeled Proteins. The rate of amino-terminal changes in A1-labeled $G\alpha_{il}$ Hexa I residues upon light activation of rhodopsin was measured by monitoring the increase in emission at 617 nm (excitation at 575 nm) of indicated labeled $G\alpha_{il}$ Hexa I subunits reconstituted with $G\beta\gamma$ (200 nM each) in the presence of dark-adapted rhodopsin (200 nM) at 21 °C both before (basal) and within seconds after activation by light, and monitored over time. The data were plotted as the emission increase compared to basal emission prior to receptor activation, and the rate was determined by plotting the data as a percent of maximal and fitting the data to an exponential association curve using Prism 4.0. The rate of changes in A1-labeled $G\alpha_{il}$ residues upon GTPγS binding was measured in a similar manner. The emission at 617 nm (excitation at 575 nm) was monitored at 21 °C both before and after addition of GTPγS (10 μM) to indicated labeled $G\alpha_{il}$ Hexa I subunits complexed with $G\beta\gamma$ (200 nM each) in the presence of light-activated rhodopsin (200 nM) for 30 min. Receptor-free nucleotide exchange (basal exchange) in the absence of rhodopsin in reconstituted heterotrimers was performed essentially as described above to yield the GTPγS spectrum, with emission monitored at 617 nm over a period of 45 min, for examination of changes in the environment of the labeled residue in the absence of ROS membranes. The data (average of three or more independent experiments) were normalized to the level of fluorescence before GTPγS addition (set to 1.0), and the rate was determined by fitting the data to an exponential dissociation curve using Prism 4.0.

Receptor-Mediated Nucleotide Exchange in Unlabeled Proteins. The rate of receptor-catalyzed nucleotide exchange was measured by monitoring the time-dependent increase in the Trp^{211} fluorescence (ex at 290 nm and em at 340 nm) of $G\alpha_{il}$ proteins reconstituted with $G\beta\gamma$ (200 nM each) in the presence of 100 nM rhodopsin (light activated) at 21 °C following the addition of GTPγS (10 μM). The data (average of three or more independent experiments) were normalized to the baseline (0%) and the fluorescence maximum (100%). The exchange rate was determined by fitting the data to an exponential association curve using Prism 4.0 (GraphPad Software).

Rhodopsin Binding Assay. The ability of labeled myristoylated and unmyristoylated $G\alpha_{il}$ proteins to bind rhodopsin in urea-washed ROS membranes was assessed by adding aliquots of the indicated labeled $G\alpha_i$ Hexa I proteins (5 μM) preincubated with an excess of $G\beta\gamma$ (10 μM) to rhodopsin (50 μM) in a buffer containing 50 mM Tris (pH 8.0), 100 mM NaCl, and 1 mM $MgCl_2$ in the dark, after light activation, with addition of GTPγS (40 μM) to a light-activated sample. Following a 30 min incubation at 4 °C,

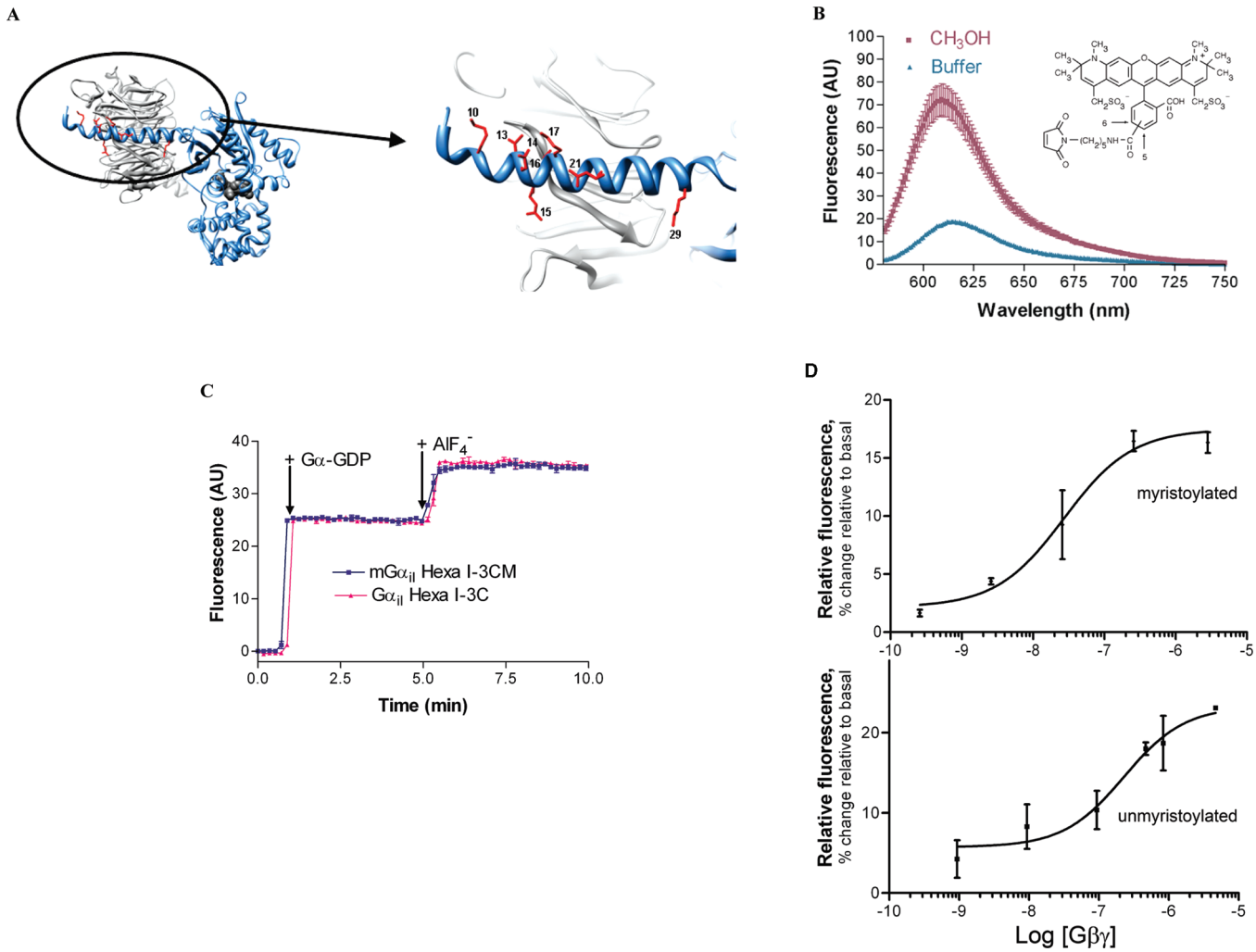

FIGURE 1: Labeling of $G\alpha_{il}$ Hexa I protein with A1 probe. (A) Location of individual Cys mutations required for subsequent thiol-directed labeling of $G\alpha_{il}$ Hexa I proteins. G_i structure from PDB entry 1GP2 (*40*), rendered with Chimera (*41*). Amino terminus of the G_i heterotrimer, with $G\beta\gamma$ colored light gray, GαGDP blue, and residues selected for labeling red. (B) A1 probe (inset) reports changes in environment. Dissolution of 10 nM A1 probe in methanol (purple) is accompanied by increased emission intensity, as compared to the same concentration of probe in aqueous buffer (teal), each scanned in triplicate (±sem). (C) A minimum of a 40% increase in intrinsic Trp^{211} fluorescence (ex at 280 nm and em at 340 nm) is seen upon AlF_4^- activation of all properly folded and functional Gα proteins, shown here for $G\alpha_{il}$ Hexa I fluorescently labeled at the third residue, in both myristoylated (blue) and unmyristoylated (pink) proteins. (D) A1-labeled $G\alpha_{il}$ Hexa I subunits bind $G\beta\gamma$. Addition of increasing amounts of $G\beta\gamma$ subunits to A1-labeled $G\alpha_{il}$ Hexa I subunits labeled at the third residue in a myristoylated (top) or unmyristoylated (bottom) protein results in a dose-dependent change in emission from labeled Gα protein upon subunit association, less background in the absence of Gα protein (percent change over basal, average of three independent measurements ± sem).

the membranes in each sample were pelleted by centrifugation at 20000*g* for 1 h, and supernatants were removed from pellets. For the dark samples, reaction mixtures were foil-protected from light until removal of the supernatant, which was performed under dim red light. The isolated supernatant and pellet fractions were boiled, resolved by SDS−PAGE, visualized with Coomassie blue, and quantified by densitometry using a BioRad Multimager. Each treatment (dark, light, and light with GTPγS) was quantified by comparison of the amount of 40 kDa $G\alpha_{il}$ proteins in either the pellet or supernatant to the sum total of Gα in both fractions, as identified by comigration with the $G\alpha_{il}$ standard, and expressed as a percentage of the total Gα present in each given sample. Data are averages of at least three independent experiments.

RESULTS

Labeling of $G\alpha_{il}$ Hexa I Proteins. To measure receptor-mediated changes in the amino terminus of $G\alpha_{il}$ proteins, in the presence and absence of myristoylation, we labeled a number of individual amino-terminal $G\alpha_{il}$ Hexa I proteins at specific side chain positions (Figure 1A). A $G\alpha_{il}$ Hexa I parent protein lacking solvent-exposed cysteines was used as a template for introduction of cysteine residues at positions indicated in Figure 1A, expressed as both myristoylated and unmyristoylated proteins. Both wild-type $G\alpha_{il}$ and $G\alpha_{il}$ Hexa I proteins, in complex with $G\beta_1\gamma_1$ ($G\beta\gamma$), can productively interact with rhodopsin [as seen in receptor-mediated GTPase and [^{35}S]GTPγS binding (*22, 27, 28*)].

Prior to using fluorescently labeled $G\alpha_{il}$ proteins as reporters of Gα environmental changes in an experimental protocol involving rhodopsin, it was necessary to select a fluorescent probe with spectral characteristics that do not overlap those of rhodopsin. Rhodopsin and its photoactivated metarhodopsin intermediates MI, MII, and MIII exhibit absorbance spectra which can interfere with many commonly used fluorescent probes. Highly conjugated probes with

excitation maxima in the far-red range (where rhodopsin and its intermediates are not affected) were therefore sought for this study. We examined three highly conjugated fluorescent probes with spectral characteristics in the far-red range: BODIPY^{595}, Atto^{610}, and Alexa^{595} (A1). Both Atto^{610} and A1 probes effectively labeled desired residues with an efficiency of labeling between 0.25 and 0.6 mol of label/mol of protein, while BODIPY labeling of Gα subunits was much less efficient (0.1 mol of label/mol of protein), likely due to the poor solubility of this probe under buffer conditions required for the maintenance of the optimal activity of Gα subunits. The Gα$_{il}$ Hexa I proteins successfully labeled with the Atto^{610} fluorescent probe underwent significant photobleaching under our assay conditions, in contrast to Gα$_{il}$ Hexa I proteins labeled with A1, which were relatively photostable. Although not all fluorescent molecules are environmentally sensitive, the A1 probe reports changes in the polarity of its environment, as free, unreactive A1 probe alone demonstrated an increased emission intensity in methanol as compared to its emission in aqueous buffer (Figure 1B).

Labeling amino-terminal residues of Gα$_{il}$ Hexa I proteins with the A1 probe does not perturb the ability of these proteins to undergo activation-dependent changes, nor does it prevent binding to Gβγ subunits, consistent with previous studies using a variety of fluorescent probes (*22, 23*). For example, in Figure 1C, activation-dependent changes induced by the transition state mimetic, AlF_4^-, result in a ≥40% increase in intrinsic tryptophan fluorescence, a prerequisite for use of the labeled proteins in these studies. Gβγ binds labeled Gα$_{il}$ Hexa I proteins; the dose-dependent changes in emission from the protein labeled at the third residue upon binding to Gβγ (Figure 1D) resulted in apparent K_d values of 30 and 230 nM for myristoylated (Figure 1D, top) and unmyristoylated (Figure 1D, bottom) proteins, respectively. These values are consistent with previously published values for the interaction between fluorescently labeled Gα$_{il}$ Hexa I subunits and Gβγ (*22, 23*), and the relatively higher affinity of Gβγ for myristoylated subunits is consistent with the known myristoylation-dependent enhancement of subunit affinity (*29*).

The Amino Terminus Reports Receptor-Mediated Changes in Environment upon Activation and GTPγS Binding. After confirming that labeled Gα$_{il}$ Hexa I proteins are properly folded and functional, we sought to determine whether these proteins could report interactions with activated, membrane-bound receptors, using an experimental protocol depicted in Figure 2A. In vivo, rhodopsin is coupled to G$_t$ activation. Both Gα$_i$ (and G$_i$ family member Gα$_t$) functionally couple to rhodopsin in vitro, and both undergo cotranslational myristoylation; however, unlike Gα$_t$, Gα$_i$ is expressed well in *E. coli*. Both myristoylated and unmyristoylated Gα$_{il}$ subunits, in complex with native, acylated Gβ$_1$γ$_1$ (Gβγ) subunits, are known to bind to rhodopsin upon light activation and to be released from the membrane upon subsequent GTP binding (*14, 20*); the goal of these studies was to examine changes in specific amino-terminal residues during this process. Therefore, emission of a fluorescently labeled Gα$_{il}$ Hexa I protein (reconstituted with Gβγ) was first scanned in the presence of ROS membranes containing dark-adapted rhodopsin, resulting in the basal (dark) emission spectrum to which later changes were then compared. Emission was scanned again after light activation (catalyzing GDP release and generating the empty pocket state), and finally after addition of GTPγS to the cuvette, which leads to dissociation from the receptor, enabling both Gα and Gβγ to interact with their respective downstream effectors. Normalizing emission from labeled G protein to that obtained in the basal (dark) states eliminates effects associated with protein−lipid interaction which occur independently of receptor activation.

Given the fact that rhodopsin is light sensitive and demonstrates multiple absorbance maxima, the probe selected for these studies must exhibit spectral characteristics in the far-red range, to prevent overlap with rhodopsin. The majority of rhodopsin absorbance (and that of its photointermediates) occurs at wavelengths below 500 nm. Studies by Imamoto et al. demonstrate that the A1 probe is compatible with assays involving rhodopsin (*30*). In control experiments to confirm this, rhodopsin was scanned from 580 to 750 nm (in the absence of labeled protein) in the dark, after light activation, and upon addition of GTPγS, with excitation at 575 nm. Rhodopsin does not substantially contribute to the overall emission signal, as seen in Figure S1A of the Supporting Information and resulting difference spectra (inset of Figure 2B). As a further control, we also measured emission changes from free probe (made unreactive by treatment with DTT) in the presence of ROS membranes, in the absence of G protein. The free, unreactive A1 probe in the presence of dark ROS showed no evidence of light- or GTPγS-dependent changes under our experimental conditions (Figure S1B of the Supporting Information).

Using the protocol depicted in Figure 2A, we examined the emission spectra of myristoylated (Figure 2B) and unmyristoylated (Figure 2C) Gα$_{il}$ Hexa I proteins labeled at the third residue in complex with Gβγ, first in the presence of inactive rhodopsin (black traces) and again upon receptor activation (red traces). Both myristoylated and unmyristoylated labeled proteins demonstrated robust changes in their environment upon receptor activation, relative to their respective environments in the inactive state. Upon receptor-mediated GTPγS binding, only the unmyristoylated protein demonstrated a decrease in fluorescence, corresponding to a relatively more solvent-exposed (aqueous) environment for the unmyristoylated amino terminus upon GTPγS binding (Figure 2C, green). The myristoylation-dependent difference in environment upon GTPγS binding is not due to the presence of membrane lipids in the experiment, as this difference is still evident in a membrane-free, receptor-free environment (Figure 2D) as a result of basal (unstimulated) nucleotide exchange. Furthermore, we confirmed the ability of this myristoylated protein to undergo GTPγS-dependent changes in solution by intrinsic Trp^{211} fluorescence, which was found to increase in a manner similar to that of the wild type upon addition of GTPγS (not shown). Therefore, there is a similar degree of solvent protection in both the heterotrimeric and GTPγS-bound state for myristoylated protein labeled at the third residue (Figure 2B,D). Together, these results are consistent with a myristoylation-dependent solvent protection of the extreme amino terminus upon GTPγS binding.

Comparison of Light- and GTP-Dependent Changes in Specific Amino-Terminal Residues of Gα$_{il}$ Proteins. We next examined relative differences in the emission of nine individually labeled amino-terminal residues during the G

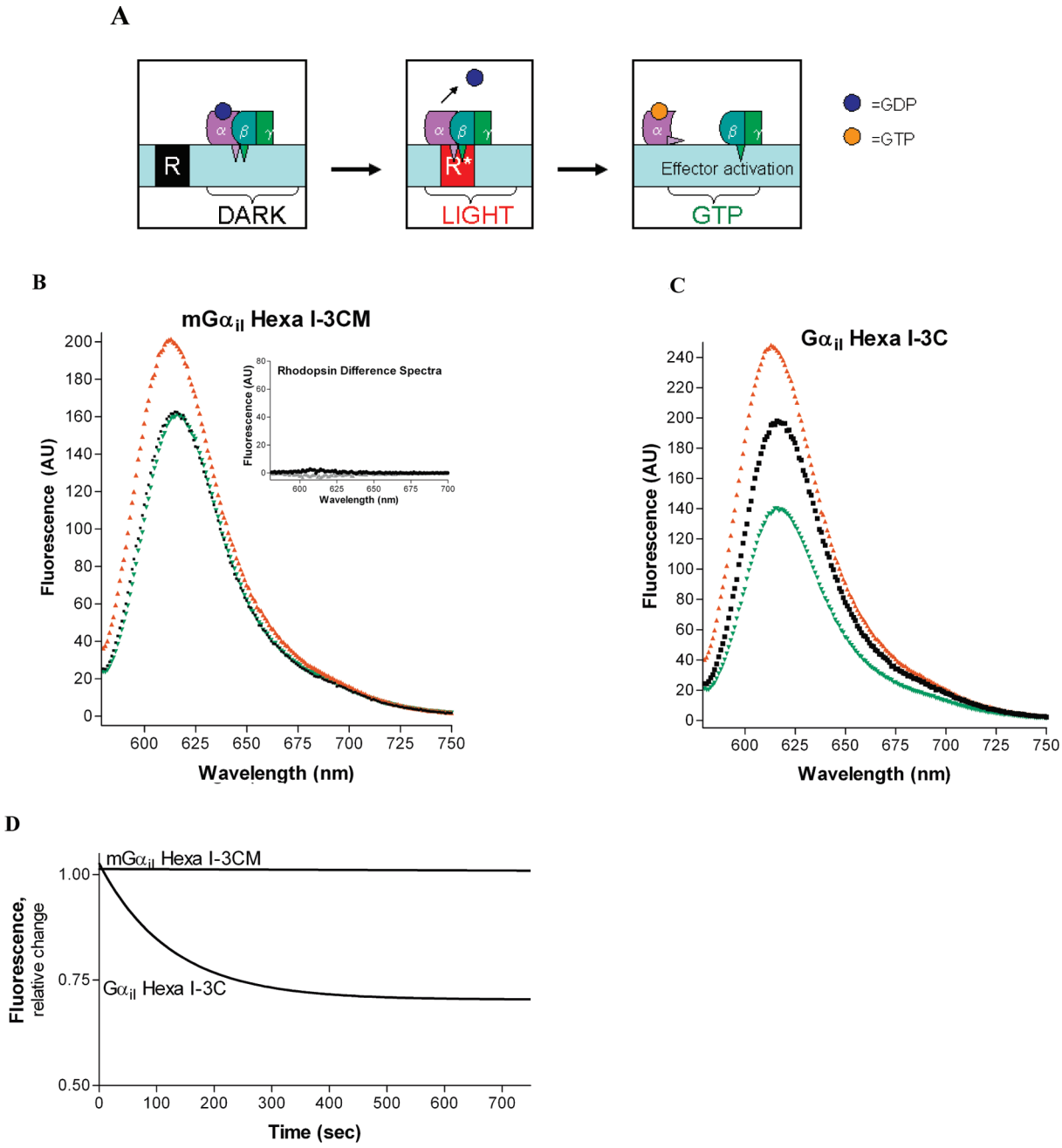

FIGURE 2: Receptor-mediated and activation-dependent changes in A1-labeled Gα_{il} Hexa I proteins. (A) Schematic of G protein activation by the membrane-bound receptor. (B and C) Activation-dependent changes (representative spectra) in the presence of rhodopsin. Gα_{il} Hexa I proteins (B, myristoylated; C, unmyristoylated) were fluorescently labeled at the third residue, reconstituted with G$\beta\gamma$, and emission was sequentially scanned (excitation at 575 nm), first in the presence of dark-adapted rhodopsin (black trace), then after light activation (red), and finally upon addition of GTPγS (green). The inset of panel B shows control difference spectra of rhodopsin alone (dark gray, light activated − dark state; light gray, light activated state − after addition of GTPγS to ROS) in the absence of G protein (raw data shown in Figure S1A of the Supporting Information). (D) Changes in emission from labeled proteins reconstituted with G$\beta\gamma$ (ex at 575 nm and em at 615 nm) upon basal GTPγS binding in the absence of ROS membranes containing rhodopsin. Emission changes are monitored over 45 min to allow for full exchange under uncatalyzed conditions. Experiments were performed in triplicate and normalized to emission prior to GTPγS addition (set to 1.0).

protein cycle in myristoylated and unmyristoylated proteins, which reflect changes in the probe's environment upon activation and deactivation. Comparison of the emission of each of the individually labeled proteins upon receptor activation and GTPγS binding (Figure 3A,B) paints a picture of the relative changes in the environment for each residue as the G protein moves from the inactive, heterotrimeric, dark state (obtained in the presence of dark-adapted ROS) to the receptor-bound empty pocket (light) state and finally to the GTPγS-bound state. Although myristoylation confers a greater degree of membrane association for heterotrimeric Gα subunits in the dark (Figure 3C,D), both myristoylated and unmyristoylated subunits efficiently translocate to membrane fractions upon light activation. Because introduction of membranes into buffer in a cuvette containing soluble G proteins can induce a small variation in signal due to scatter, we set the basal emission of the labeled proteins in the presence of dark-adapted ROS to 1.0; all subsequent changes were normalized to basal. This protocol accounts for contributions to basal emission from membrane association

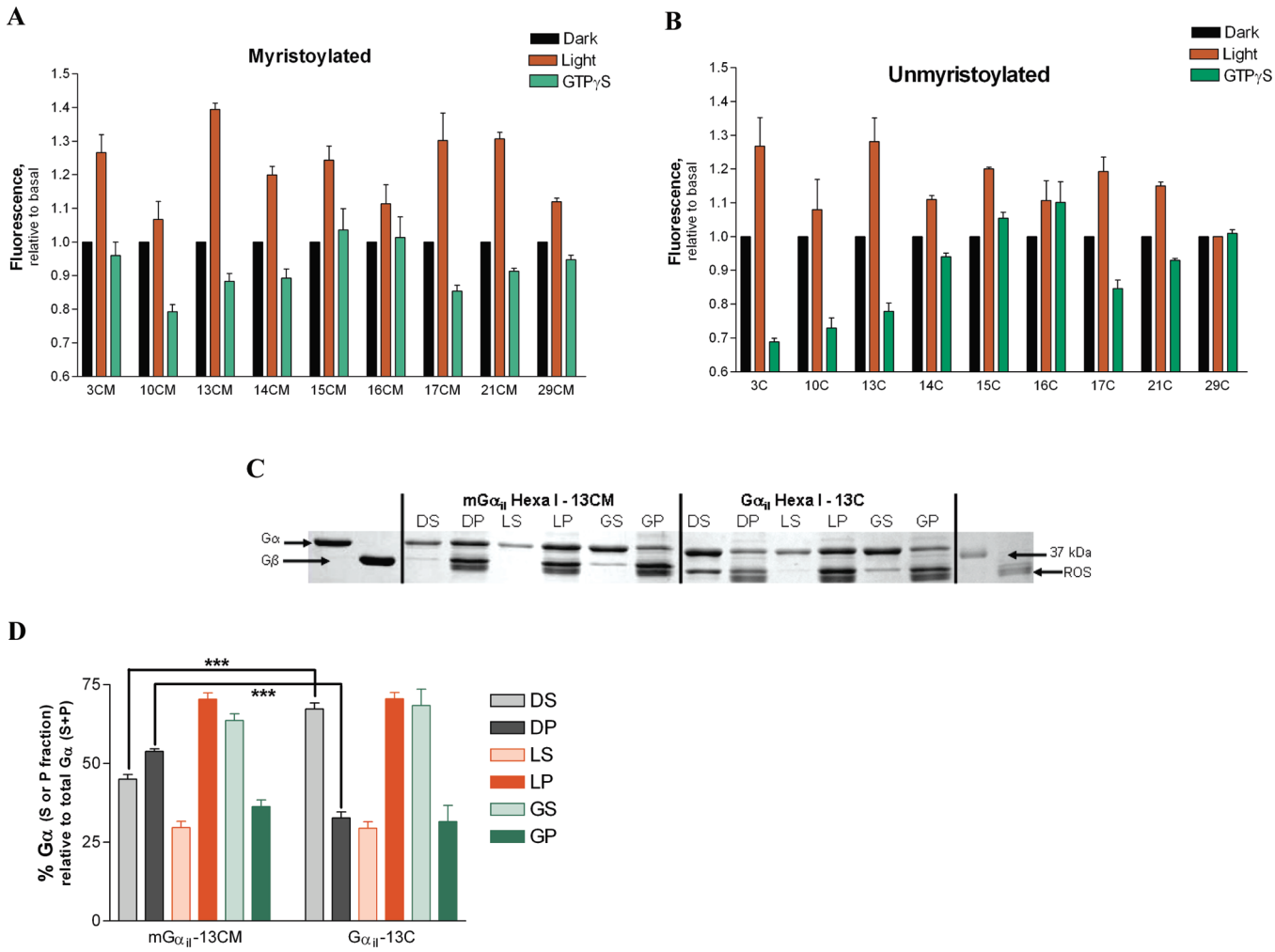

FIGURE 3: Amino-terminal residues of Gα$_{il}$ Hexa I proteins report specific receptor-dependent changes in environment. (A and B) Gα$_{il}$ Hexa I proteins (myristoylated, A; unmyristoylated, B) were fluorescently labeled at the indicated residue and reconstituted with G$\beta\gamma$, and emission was sequentially scanned (excitation at 575 nm), first in the presence of dark-adapted rhodopsin (black bars, normalized to 1.0), then after light activation (red bars), and finally upon addition of GTPγS (green bars). Results are from three or more independent experiments (±sem), each performed in duplicate. (C) Rhodopsin binding assay. Representative SDS−PAGE (Coomassie stain) analysis of Gα$_{il}$ Hexa I proteins labeled at the 13th residue, reconstituted with an excess of G$\beta\gamma$ prior to binding to ROS in the dark (D), in the light (L), and after light activation followed by addition of GTPγS (G). S denotes the supernatant fraction, and P denotes the fraction from the pellet after centrifugation. (D) Quantitation of membrane binding experiments, average of three independent experiments (±sem; $p < 0.0001$). Asterisks demonstrate a significant increase in the level of membrane association for myristoylated Gα in complex with G$\beta\gamma$ in the presence of dark rhodopsin.

of myristoylated proteins in the dark, as well as small variations in labeling efficiencies at different residues.

Since the A1 probe demonstrates decreased emission intensity in a more aqueous environment and increased intensity in a more hydrophobic environment (Figure 1B), the receptor-mediated increases in emission upon light activation from the labeled proteins (Figure 3A,B) likely represent increases in the hydrophobicity of the environment detected by the fluorescent probe. The intensities exhibited for the labeled proteins are shown relative to that detected for each in the inactive, heterotrimeric state [as measured in the presence of ROS membranes containing dark-adapted rhodopsin (Figure 3A,B, black bars, and Figure 2A, left panel)]. The light-activated state shown by the red bars in Figure 3 effectively represents the receptor-bound, empty pocket conformation depicted in the center panel of Figure 2A. Light activation is accompanied by increased emission intensity at nearly all positions examined along the amino-terminal helix (Figure 3A,B, red bars), as compared to their inactive, heterotrimeric states (black bars). Light-dependent changes in fluorescence were accompanied by enhanced membrane association (where the relative percentage of Gα in the pelleted fraction exceeds the percentage of Gα in the soluble fraction) for both myristoylated and unmyristoylated proteins (Figure 3C,D), consistent with activation-mediated binding of labeled proteins to membrane-bound receptors. This localization is reversed by addition of GTPγS (Figure 3A,B, green bars) to the light-activated samples, indicating increased solubility upon GTPγS binding.

The light-dependent changes in fluorescence ranged from a 25 to 40% increase in emission over basal upon light activation of the receptor in myristoylated proteins labeled at the third, 13th, 17th, and 21st residues (Figure 4A). Myristoylation-dependent differences in emission intensity were statistically significant at several positions (Figure 4A). These changes (and those related to receptor-mediated GTPγS binding) are eliminated when labeled G proteins are boiled prior to use in the assay (10 min at 95 °C). The emission changes in G proteins which occur after light is flashed on the system are also ablated when heat-denatured

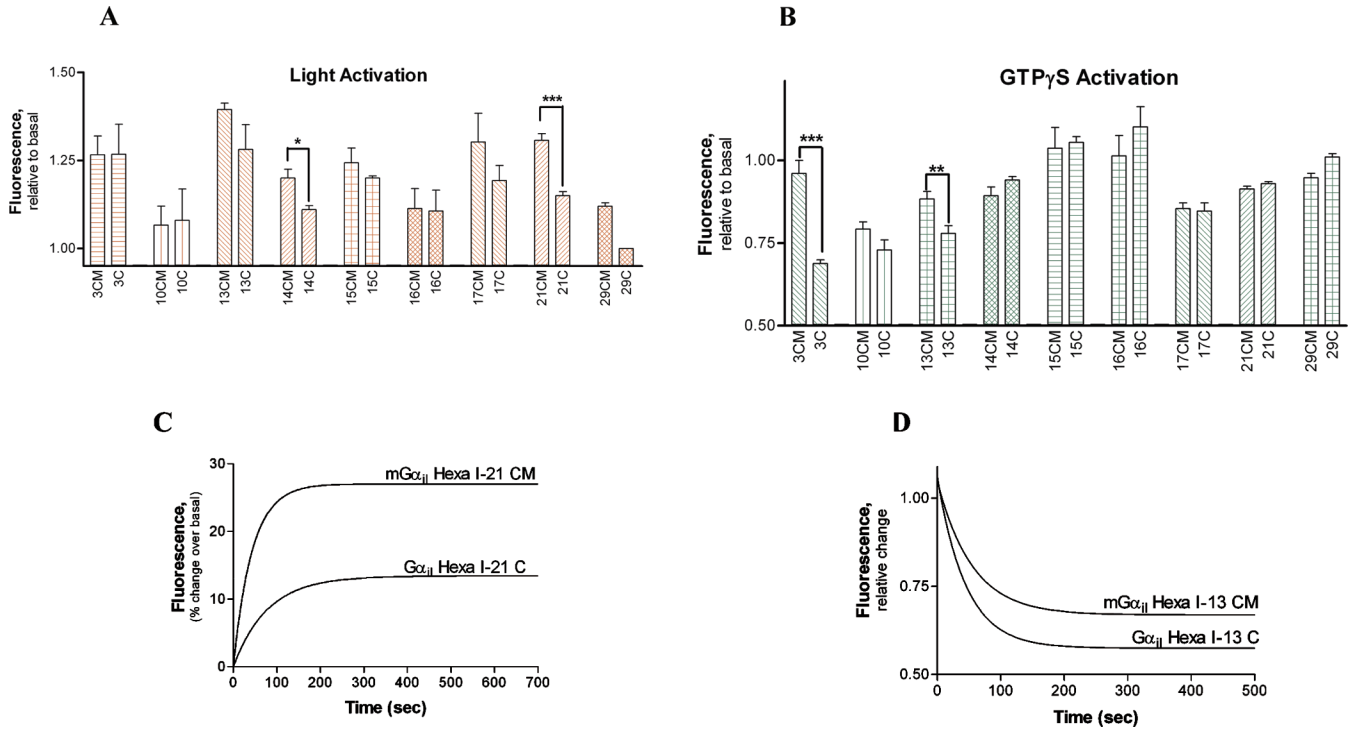

FIGURE 4: Comparison of receptor-mediated changes in myristoylated and unmyristoylated labeled proteins. Direct comparison of light-dependent intensity changes (A) and GTPγS-dependent intensity changes (B) from panels A and B of Figure 3 (one asterisk indicates $p < 0.01$; two asterisks indicate $p < 0.001$; three asterisks indicate $p < 0.0001$). (C and D) Time dependence of receptor-mediated changes in emission of myristoylated and unmyristoylated proteins (ex at 575 nm and em at 615 nm, average of three or more independent experiments). (C) Time-dependent change upon light activation for protein labeled at the 21st residue relative to the GDP-bound, inactive state (set to 0) and measured immediately after light activation. (D) Time dependence of GTPγS-mediated changes in emission of myristoylated and unmyristoylated protein labeled at the 13th residue in the presence of light-activated receptor immediately after addition of GTPγS as described in Materials and Methods, compared to the level of emission in the light-activated state (set to 1.0).

ROS membranes (10 min at 95 °C) are substituted for ROS membranes kept at 4 °C in the experiment (in conjunction with properly folded G proteins). The lack of light-dependent changes exhibited after heat denaturation of either G proteins or rhodopsin suggests the changes observed are directly related to the proper folding and functioning of these proteins.

While enhanced membrane localization of myristoylated proteins might be predicted to mediate the increases in intensity upon light activation, it is important to keep in mind that these changes are relative to their environment in the dark state. Both myristoylated and unmyristoylated proteins efficiently translocate to membrane fractions upon light activation, with the myristoylated proteins demonstrating a significantly higher degree of membrane association in the dark state than unmyristoylated (Figure 3C,D), which results in a smaller relative difference between the dark and light membrane localization for myristoylated proteins, and likewise a larger difference between these two states for the unmyristoylated protein. If membrane localization was solely responsible for light-dependent changes in emission, then the myristoylated proteins would be predicted to exhibit a smaller difference in emission upon light activation than the unmyristoylated protein. However, this is not the case. This argues against membrane translocation as the cause of the myristoylation-dependent enhancement of emission we observe upon receptor activation.

Although this study is focused on the relationship between membrane-bound receptors and amino-terminal residues of $G\alpha_{il}$ proteins and although detergents would be expected to weaken interactions between membrane-bound receptors and myristoylated proteins, we investigated the role of membrane lipids in this system using a detergent-solubilized form of rhodopsin and labeled, myristoylated $G\alpha_{il}$ Hexa I proteins. The labeled proteins retained the ability to report changes in emission upon light activation of receptors, albiet to a slightly lesser extent compared to that seen using intact ROS membranes, which were eliminated by heating the soluble rhodopsin preparation for 10 min at 95 °C prior to use in these experiments (Figure S2 of the Supporting Information).

We further characterized the time dependence of the increase in emission upon light activation from myristoylated and unmyristoylated proteins labeled at the 21st residue (Figure 4C), which differed significantly upon receptor activation (Figure 4A). The rate of the light-dependent change is considerably faster for the myristoylated protein ($0.023\ s^{-1}$), in comparison to that of its unmyristoylated counterpart ($0.012\ s^{-1}$). These results suggest myristoylation can enhance both the rate and intensity of receptor-catalyzed changes in fluorescence emission seen upon light activation.

Finally, binding of GTPγS increased the solvent exposure of nearly all of the residues along the amino terminus (Figure 3A,B, green bars vs red bars) as compared to their environment in the light-activated state. Myristoylation dramatically inhibited the GTPγS-mediated change in solvent exposure at position 3 and had a more subtle effect at residues 10 and 13 (Figure 4B). We characterized the time dependence of the decrease in emission intensity upon GTPγS binding at the 13th residue (Figure 4D), which was significantly altered by myristoylation as seen in Figure 4B. The rate of change in emission which accompanies GTPγS binding in the

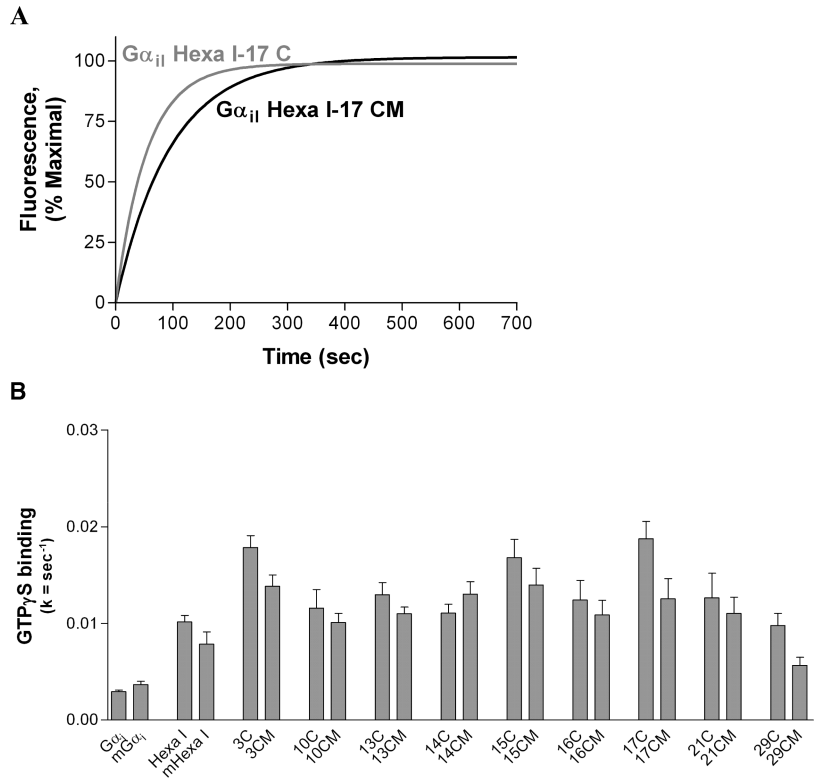

FIGURE 5: Comparison of receptor-mediated changes in unlabeled proteins reported by intrinsic Trp^{211} fluorescence. (A) Emission of Gα$_{il}$ Hexa I-17C (unmyristoylated, gray) and -17CM (myristoylated, black) in complex with Gβγ is monitored (ex at 290 nm and em at 340 nm) after addition of GTPγS in the presence of activated rhodopsin, compared to the level prior to addition of GTPγS, as described in Materials and Methods. (B) Receptor-mediated exchange rates measured for each individual Gα$_{il}$ Hexa I mutant protein. The exchange rates were determined by fitting each data set to an exponential association curve. Data represent the averages of four to six independent experiments (±sem).

presence of the light-activated receptor shown in Figure 4D was nearly the same for myristoylated and unmyristoylated labeled proteins (0.018 and 0.022 s^{-1}, respectively), a similarity which is confirmed using unlabeled proteins, described below. Therefore, myristoylation-dependent differences in emission intensity which accompany GTPγS binding do not necessarily result in differences in the rates of GTPγS binding from the labeled proteins.

Myristoylation Does Not Enhance Receptor-Mediated Nucleotide Exchange of Gα$_{il}$ Hexa I Proteins As Measured by the Intrinsic Trp^{211} Fluorescence in Unlabeled Proteins. As we detected no significant differences in the rates of GTPγS binding in labeled proteins (despite some differences in intensity), we confirmed this finding by comparison of these rates in unlabeled proteins (Figure 5). This was accomplished by taking advantage of the fact that the intrinsic tryptophan fluorescence emission (reported by Trp^{211} located in the switch II region) increases upon GTPγS binding, and the time dependence of this increase can be measured in the presence of light-activated rhodopsin (*14*) which is able to catalyze nucleotide exchange in G$_i$ (as well as G$_t$) proteins. The Gα$_{il}$ Hexa I−Gβγ complex is known to undergo a rate of nucleotide exchange slightly higher than that of wild-type Gα$_{il}$βγ (*14*), shown in Figure 5B for comparison. This effect is due to conservative replacement of native solvent-exposed cysteines, a prerequisite for the generation of the cysteine-depleted Gα$_{il}$ Hexa I parent protein, previously shown to have functional activities similar to that of wild-type Gα$_{il}$ (*22, 23*). Receptor-mediated nucleotide exchange rates for myristoylated and unmyristoylated proteins reveal no significant differences in the rates of nucleotide exchange for myristoylated proteins and unmyristoylated Gα$_{il}$ Hexa I proteins (Figure 5A,B), similar to results obtained with labeled Gα$_{il}$ Hexa I proteins. Furthermore, the slightly higher (but statistically indistinct) rate of receptor-mediated nucleotide exchange in unmyristoylated proteins is not likely a result of an increased level of basal exchange, as the exchange rate of unmyristoylated Gα$_{il}$ Hexa I-3C (Figure 2D) is 0.007 s^{-1}, which is one-third of the receptor-catalyzed rate (Figure 5B). Therefore, it is unlikely that receptor-independent activation of Gα is a major contributor to exchange rates in these unmyristoylated proteins. The ability of unmyristoylated proteins to undergo efficient receptor-mediated nucleotide exchange also confirms that myristoylation is not a requirement for productive interaction with membrane-bound receptors, consistent with results from these and other published studies (both in vitro and in vivo) (*20, 21*).

Changes in Fluorescence Emission Intensity Are Accompanied by Shifts in Emission Maxima of Labeled Proteins upon Receptor Activation and GTPγS Binding. Closer examination of the emission maxima (em$_{max}$) of the free A1 probe in aqueous buffer solution versus emission in a more hydrophobic environment such as methanol (Figure 1B) reveals a small but reliable shift of the em$_{max}$ to lower wavelengths (blue-shifted emission) in a less aqueous environment, when plotted as percent of each of their respective maximum intensities (Figure 6, top panel). The em$_{max}$ of an equimolar amount of free A1 probe shifted from 617 nm in aqueous buffer to 609 nm in methanol, a change of 8 nm. The emission of A1-labeled proteins also demon-

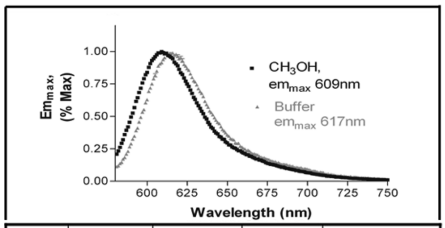

Em$_{max}$	Dark (D)	Light (L)	D-L	GTPγS
3C	616.20	613.34	2.8	616.43
3CM	614.12	611.56	2.6	615.78
10C	617.01	615.13	1.9	616.25
10CM	617.00	615.79	1.2	617.00
13C	617.36	612.91	4.3	617.12
13CM	614.09	610.47	3.6	616.75
14C	614.31	613.73	0.6	615.22
14CM	614.67	613.02	1.7	616.44
15C	616.01	615.54	0.5	616.37
15CM	616.82	616.12	0.7	617.41
16C	616.43	614.97	1.5	615.79
16CM	616.26	614.86	1.4	616.72
17C	616.69	613.67	3.1	616.98
17CM	615.61	612.45	3.2	616.98
21C	616.59	614.24	2.3	616.82
21CM	616.27	612.95	3.3	616.40
29C	616.26	615.71	0.6	616.58
29CM	617.07	615.69	1.3	617.19

FIGURE 6: A1 probe reports environmentally dependent changes in emission maxima. (Top) Free, unreactive, A1 probe (10 nM) undergoes an 8 nm blue shift in methanol (black trace) vs aqueous buffer (gray), with respective intensities normalized to 100%. (Bottom) Intensity changes for labeled Gα_{il} Hexa I proteins accompanied by a shift in emission maxima (in nanometers, average of three independent measurements) upon receptor activation and GTPγS binding. The third column (D-L) is the net blue shift for each labeled protein upon light activation, obtained by $em_{max\ dark} - em_{max\ light}$ (in nanometers).

strated a small but detectable blue shift upon receptor activation, on the order of 1−4 nm, which are reversed by GTPγS binding (Figure 6). Closer examination of the magnitude of these shifts reveals a relatively greater blue shift for proteins labeled at the third, 13th, 17th, and 21st residues. While this probe reports more robust changes in overall emission intensity than in the relative smaller shifts seen in emission maxima, the intensity changes (Figure 3A,B) are generally consistent with blue shifts seen upon light activation, which are reversed by GTPγS binding (Figure 6).

DISCUSSION

Biophysical studies have broadened our understanding of receptor-mediated G protein activation and, in combination with crystal structures, provide powerful tools for probing G protein signaling. The most complete crystallographic views of Gα amino-terminal structure have been obtained with unmyristoylated Gα proteins in complex with G$\beta\gamma$, which shows the Gα amino-terminal α-helix making extensive contacts with G$\beta\gamma$ (Figure 1A). Since isolated Gα proteins are unstable in the nucleotide-free state and since there is no high-resolution structure of an activated receptor in complex with a G protein, biophysical studies offer unique insights into the conformation of the receptor-bound, empty pocket state of Gα subunits. Our results demonstrate that residues all along the amino-terminal helix of Gα_{il} Hexa I proteins undergo specific receptor-mediated changes upon activation. These changes map to a distinct surface of the amino-terminal helix, suggesting intimate involvement of the amino terminus of Gα in changes that accompany receptor-mediated G protein activation processes. While these data do not rule out contributions from membrane lipids in receptor-mediated amino-terminal environmental changes observed in Gα_{il} Hexa I proteins, such contributions are secondary to receptor activation, as heat denaturation of rhodopsin (as well as heat denaturation of soluble rhodopsin) eliminates these changes, and because these changes persist in the presence of detergent-solubilized receptors.

The fluorescent probe linked to individual amino-terminal Gα_{il} Hexa I residues reports changes in its environment during signaling. The current data, including observations that the amino terminus can cross-link to activated receptors (*17*) and the ability of amino-terminal peptides to compete with Gα_t for stabilization of activated rhodopsin (*16*), are altogether consistent with a specific interaction between amino-terminal residues of Gα and activated receptors. These interactions result in changes in the environment of individually labeled residues.

In the heterotrimeric (basal) state, this environment is depicted in dark spectra, which are obtained in the presence of the membrane-bound, inactive receptor. The light spectra, obtained after light activation of the receptor and before GTPγS addition, generate the receptor-bound, empty pocket conformation. The light-activated emission spectra reflect changes in the environment of the probe linked to individual amino-terminal residues that occur upon receptor-mediated G protein activation. Myristoylation enhanced not only the intensity but also the rate of the light-mediated changes in emission upon light activation. The myristoylation-dependent increase in the rate of light-dependent emission changes may be due to enhanced G protein binding to ROS in the dark state, as increased G protein membrane localization prior to light activation would reduce the factors affecting the rate of light activation from a three-dimensional to a two-dimensional diffusion issue.

The increases in intensities upon light activation, accompanied by blue-shifted emission maxima, together indicate a less aqueous accessible environment upon receptor activation. Furthermore, several of the residues which demonstrate both the greatest emission shifts and intensity changes upon receptor activation (residues 13, 17, and 21) map to a distinct face of the Gα amino-terminal α-helix (Figure 7A) located opposite the G$\beta\gamma$ binding interface (Figure 7B). The native residues at positions 13, 17, and 21 (V, K, and R, respectively) in Gα_i proteins would be predicted to promote membrane interactions through hydrophobic and electrostatic interactions, which may augment interactions of G proteins with membrane-bound receptors in vivo. Despite the fact that mutation to cysteine and addition of the A1 probe did not perturb the ability of the labeled proteins to undergo activation-dependent changes, to bind G$\beta\gamma$, to exchange nucleotide, or to report activation-dependent changes, it is not unreasonable to expect that unlabeled, native proteins may interact even better with membrane-bound receptors than the labeled proteins used in this study. Nevertheless, since heat denaturation of the labeled proteins eliminated their ability to detect changes in

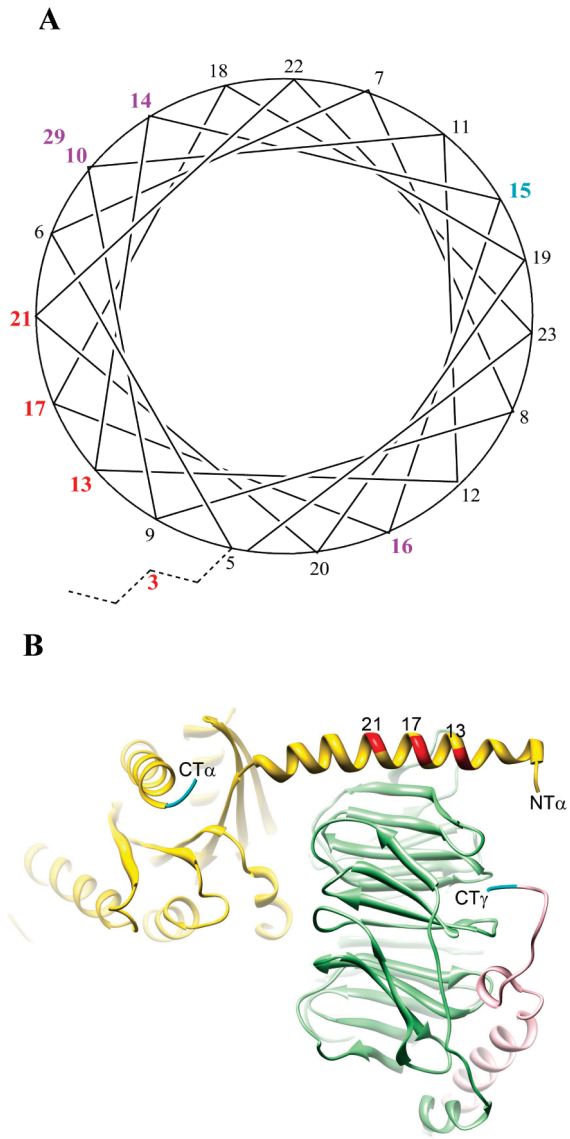

FIGURE 7: Receptor-mediated changes map to a distinct surface of the Gα$_i$ amino-terminal helix. (A) Helical wheel depiction of ordered residues in the amino terminus of Gα$_i$ as seen in the G$_i$ heterotrimer [PDB entry 1GP2 (*39*)], with disordered extreme amino-terminal residues shown with dotted lines. Residue numbers are colored according to receptor-mediated blue shifts in em$_{max}$ of myristoylated protein: red, >2 nm blue shift; purple, 1−2 nm; teal, <1 nm. (B) G$_i$ heterotrimer featuring the face of G$_i$ implicated in binding to the membrane-bound receptor [structure from PDB entry 1GP2 (*39*), rendered with Chimera (*40*)]. Gα is colored yellow, Gβ green, and Gγ pink, with the last ordered residues in the C-terminus of Gα (residue 347) and Gγ (residue 61) labeled CTα and CTγ, respectively, and colored teal. Red indicates residues 13, 17, and 21 in the amino-terminal helix of the Gα subunit.

their environment, as did heat denaturation of the rhodopsin preparations, this suggests the changes we observe are a result of G protein−receptor coupling between functional proteins.

Receptor activation induces release of GDP and binding of GTP, thus lowering the affinity of activated Gα subunits for receptors. This is reflected by a decrease in emission for nearly all of the A1-labeled proteins upon GTPγS binding relative to the light-activated state, and this decrease is generally more pronounced for unmyristoylated proteins, suggesting myristoylation reduces the level of aqueous exposure of amino-terminal residues in the GTPγS-bound state. This was unrelated to the presence of membrane lipids, as a similar decrease in emission was noted after basal (uncatalyzed) nucleotide exchange occurred in solution (Figure 2D). The relatively greater degree of aqueous exposure for several of the unmyristoylated proteins compared to their myristoylated counterparts upon GTPγS binding is consistent with previous EPR studies of unmyristoylated Gα$_{il}$ Hexa I proteins, which show a dramatic transition toward disorder at the amino terminus upon addition of GTPγS to the receptor−G protein complex (*22*). Solution studies of GDP-bound myristoylated Gα$_i$ Hexa I proteins reveal a relatively immobilized EPR spectra for individual residues all along the amino terminus, even in the absence of Gβγ (*23*), unlike the more mobile amino-terminal residues seen in unmyristoylated Gα$_{il}$ Hexa I proteins (*22*). Previous fluorescence studies of these isolated, labeled, myristoylated proteins in solution indicated that the amino terminus in the activated, GDP-AlF_4^--bound state is in a more hydrophobic environment than the inactive, GDP-bound state (*23*). A solvent protection of the myristoylated amino terminus via an (unidentified) intramolecular binding site would explain the relatively similar recovery we observe of myristoylated and unmyristoylated GTPγS-bound protein in the soluble fraction after centrifugation.

A number of proteins are known to utilize myristoyl switching mechanisms to regulate signaling, including recoverin, the PKA catalytic subunit, MARCKS, and ARF, with ARF's myristoyl switch triggered by GTP binding. Membrane lipids affect the nucleotide binding of a full-length ARF, but not an amino-terminally truncated (unmyristoylated) Arf protein, and a myristoylated amino-terminal peptide derived from the ARF protein also inhibited ARF activities (*44*). Myristoylation of Gα proteins may serve an analogous switching function in heterotrimeric G$_i$ proteins, mediating association with membrane-bound receptors (in concert with acylation of Gγ). Myristoylation may regulate solubility of individual Gα-GTP subunits as they dissociate from membrane-bound receptors by protecting the myristoylated amino terminus of the GTP-bound subunit from the aqueous solvent through an intramolecular binding site on the surface of the protein. The current study reveals a myristoylation-dependent solvent protection for the extreme amino terminus of Gα$_{il}$ after receptor-mediated GTPγS binding. Further work to unambiguously identify a potential intramolecular binding site for the myristoylated amino terminus of Gα$_{il}$ is currently underway.

There is a vast amount of data supporting GPCR dimerization and oligomerization, both in vitro and in vivo (reviewed in refs *31* and *32*). Although the work presented here is not aimed at addressing the question of receptor:G protein stoichiometry, it is interesting to consider a role for the myristoylated amino terminus in receptor dimerization. A dimeric receptor provides a plausible explanation for the ability of an activated receptor to cross-link to spans of residues in both the carboxy and amino terminus of Gα$_t$ (*17, 33*) with chemical and photoactivatable cross-linkers. These regions are separated by as much as 28 Å, as seen in the crystal structure of the inactive G$_t$ heterotrimer (PDB entry 1GOT). The carboxy-terminal eighth helix of rhodopsin (often called the fourth cytoplasmic loop of rhodopsin) is also known to be involved in transducin coupling through both its amino and carboxyl terminus, as

seen in peptide studies and site-directed mutagenesis of this region (*34*−*36*).

Structural studies have confirmed that the length of an entire heterotrimeric G protein is sufficient to span a receptor dimer, using crystallographic constraints from G proteins, rhodopsin, and the recently determined β-adrenergic receptor (*2, 10, 33*). Results from atomic force microscopy support a dimeric model of rhodopsin (*33*) and are also consistent with higher-order structures, which is not unlikely in vivo, given the density of receptors in the rod outer segment. The existence of GPCR dimers is supported by results from small angle neutron scattering which suggested that leukotriene B4 receptor-1, BLT1 (a member of the rhodopsin family of GPCRs), assembles with G_i proteins in a 2:1 receptor:G protein ratio upon agonist activation, using receptors stabilized in detergent solution (*37*). Recent reports suggest rhodopsin dimerization may play roles distinct from activation in vivo, as monomeric rhodopsin is sufficient for G protein activation in vitro (*43*).

While little about the functional coupling of specific residues in the amino terminus of Gα proteins to activated receptors has been published, the carboxy terminus of Gα proteins has been more extensively characterized in terms of GPCR interactions. Recent work shows that GPCR activation is coupled to a rotation and translation of the α5 helix in the carboxy terminus of $G\alpha_{il}$ Hexa I proteins, which may aid in GDP release, as elimination of this movement by a flexible linker significantly impairs receptor-mediated nucleotide exchange (*14*). Crystal structures of isolated Gα subunits (unmyristoylated) place residues within the carboxy terminus (residue 345) and the last resolved residues in the amino terminus (residue 33) into the proximity of each other. The amino-terminal portion of Gα (and its proximity to the carboxy terminus) has also been implicated in the specificity of receptor coupling in functional assays using a chimeric approach. The region which links the amino-terminal α-helix to the first β-sheet of the GTPase domain (residues 31−33 in $G\alpha_i$) is proximal to the carboxy terminus in Gα crystal structures, and this linker was shown to be of particular importance to the specificity of receptor coupling, using a $G\alpha_{15/16}$ chimera (*38*). This is consistent with the idea that the amino and carboxy termini work together in concert to effect nucleotide release upon receptor activation.

The lever arm model of receptor-mediated nucleotide release proposed by Iiri et al. (*39*) implicates a receptor-mediated amino-terminal conformational change in Gα which rotates Gα away from G$\beta\gamma$, thus distorting the nucleotide binding site and opening an exit route for GDP release. However, the functional redundancy of farnesylation of Gγ and myristoylation Gα in receptor-mediated G protein activation does not support this lever arm model of G protein activation. Furthermore, although our data are consistent with a role for the amino terminus of $G\alpha_{il}$ in receptor-mediated G protein activation, the data do not directly address the contribution from G$\beta\gamma$. Nevertheless, this work provides convincing evidence of the intimate contact between the amino terminus of $G\alpha_{il}$ and activated, membrane-bound receptors, indicated by the receptor-mediated change in the environment of the amino terminus. More intensive studies detailing changes in the spatial relationship among Gα, G$\beta\gamma$, and the receptor (and the order of such changes) leading to nucleotide release must be undertaken to fully elucidate the complete mechanism of receptor-mediated nucleotide release leading to G protein activation.

Altogether, this study identifies specific receptor-mediated changes occurring along the amino terminus, many of which are distinctly affected by myristoylation, and a myristoylation-dependent solvent protection of the extreme amino terminus of $G\alpha_{il}$ proteins after receptor-mediated G protein activation. This work paints a picture of a conformationally adaptable myristoylated amino-terminal region of Gα proteins. Myristoylation-dependent variations in the environment and conformation of amino-terminal residues of $G\alpha_{il}$ proteins upon G protein activation may play a role regulating interactions with G$\beta\gamma$, membrane-bound receptors, and soluble effectors.

ACKNOWLEDGMENT

Molecular graphics images were produced using the UCSF Chimera package from the Computer Graphics Laboratory [University of California, San Francisco, CA (supported by NIH Grant P41 RR-01081)]. We acknowledge Dr. Songhai Chen for insightful comments and R. Beavins for careful reading of the manuscript.

SUPPORTING INFORMATION AVAILABLE

Supplementary figures show additional experimental controls. This material is available free of charge via the Internet at http://pubs.acs.org.

REFERENCES

1. Noel, J. P., Hamm, H. E., and Sigler, P. B. (1993) The 2.2 Å crystal structure of transducin-α complexed with GTPγS. *Nature 366*, 654–663.
2. Lambright, D. G., Sondek, J., Bohm, A., Skiba, N. P., Hamm, H. E., and Sigler, P. B. (1996) The 2.0 Å crystal structure of a heterotrimeric G protein. *Nature 379*, 311–319.
3. Coleman, D. E., Berghuis, A. M., Lee, E., Linder, M. E., Gilman, A. G., and Sprang, S. R. (1994) Structures of Active Conformations of $G_{i\alpha1}$ and the Mechanism of GTP Hydrolysis. *Science 265*, 1405–1412.
4. Sondek, J., Lambright, D. G., Noel, J. P., Hamm, H. E., and Sigler, P. B. (1994) GTPase mechanism of G proteins from the 1.7-Å crystal structure of transducin α•GDP•AlF_4^-. *Nature 372*, 276–279.
5. Mixon, M. B., Lee, E., Coleman, D. E., Berghuis, A. M., Gilman, A. G., and Sprang, S. R. (1995) Tertiary and Quaternary Structural Changes in $G_{i\alpha1}$ Induced by GTP Hydrolysis. *Science 270*, 954–960.
6. Sondek, J., Bohm, A., Lambright, D. G., Hamm, H. E., and Sigler, P. B. (1996) Crystal structure of a G-protein $\beta\gamma$ dimer at 2.1 Å resolution. *Nature 379*, 369–374.
7. Tesmer, J. J., Berman, D. M., Gilman, A. G., and Sprang, S. R. (1997) Structure of RGS4 Bound to AlF_4^--activated $G_{i\alpha1}$: Stabilization of the Transition State for GTP Hydrolysis. *Cell 89*, 251–261.
8. Palczewski, K., Kumasaka, T., Hori, T., Behnke, C. A., Motoshima, H., Fox, B. A., Le Trong, I., Teller, D. C., Okada, T., Stenkamp, R. E., Yamamoto, M., and Miyano, M. (2000) Crystal Structure of Rhodopsin: A G Protein-Coupled Receptor. *Science 289*, 739–745.
9. Salom, D., Lodowski, D. T., Stenkamp, R. E., Le Trong, I., Golczak, M., Jastrzebska, B., Harris, T., Ballesteros, J. A., and Palczewski, K. (2006) Crystal structure of a photoactivated deprotonated intermediate of rhodopsin. *Proc. Natl. Acad. Sci. U.S.A. 103*, 16123–16128.
10. Cherezov, V., Rosenbaum, D. M., Hanson, M. A., Rasmussen, S. G., Thian, F. S., Kobilka, T. S., Choi, H. J., Kuhn, P., Weis, W. I., Kobilka, B. K., and Stevens, R. C. (2007) High-resolution crystal structure of an engineered human β2-adrenergic G protein-coupled receptor. *Science 318*, 1258–1265.

11. Graf, R., Mattera, R., Codina, J., Estes, M. K., and Birnbaumer, L. (1992) A truncated recombinant α subunit of Gi3 with a reduced affinity for $\beta\gamma$ dimers and altered guanosine 5′-3-O-(thio)triphosphate binding. *J. Biol. Chem. 267*, 24307–24314.
12. Navon, S. E., and Fung, B. K. (1987) Characterization of transducin from bovine retinal rod outer segments. Participation of the amino-terminal region of Tα in subunit interaction. *J. Biol. Chem. 262*, 15746–15751.
13. Dratz, E. A., Furstenau, J. E., Lambert, C. G., Thireault, D. L., Rarick, H., Schepers, T., Pakhlevaniants, S., and Hamm, H. E. (1993) NMR structure of a receptor-bound G-protein peptide. *Nature 363*, 276–281.
14. Oldham, W. M., Van Eps, N., Preininger, A. M., Hubbell, W. L., and Hamm, H. E. (2006) Mechanism of the receptor-catalyzed activation of heterotrimeric G proteins. *Nat. Struct. Mol. Biol. 13*, 772–777.
15. Onrust, R., Herzmark, P., Chi, P., Garcia, P. D., Lichtarge, O., Kingsley, C., and Bourne, H. R. (1997) Receptor and $\beta\gamma$ Binding Sites in the α Subunit of the Retinal G Protein Transducin. *Science 275*, 381–384.
16. Hamm, H. E., Deretic, D., Arendt, A., Hargrave, P. A., Koenig, B., and Hofmann, K. P. (1988) Site of G Protein Binding to Rhodopsin Mapped with Synthetic Peptides from the α Subunit. *Science 241*, 832–835.
17. Itoh, Y., Cai, K., and Khorana, H. G. (2001) Mapping of contact sites in complex formation between light-activated rhodopsin and transducin by covalent crosslinking: Use of a chemically preactivated reagent. *Proc. Natl. Acad. Sci. U.S.A. 98*, 4883–4887.
18. Kostenis, E., Degtyarev, M. Y., Conklin, B. R., and Wess, J. (1997) The N-terminal extension of Gαq is critical for constraining the selectivity of receptor coupling. *J. Biol. Chem. 272*, 19107–19110.
19. Bigay, J., Faurobert, E., Franco, M., and Chabre, M. (1994) Roles of Lipid Modifications of Transducin Subunits in Their GDP-Dependent Association and Membrane Binding. *Biochemistry 33*, 14081–14090.
20. Herrmann, R., Heck, M., Henklein, P., Hofmann, K. P., and Ernst, O. P. (2006) Signal transfer from GPCRs to G proteins: Role of the Gα N-terminal region in rhodopsin-transducin coupling. *J. Biol. Chem. 281*, 30234–30241.
21. Kerov, V., Rubin, W. W., Natochin, M., Melling, N. A., Burns, M. E., and Artemyev, N. O. (2007) N-Terminal fatty acylation of transducin profoundly influences its localization and the kinetics of photoresponse in rods. *J. Neurosci. 27*, 10270–10277.
22. Medkova, M., Preininger, A. M., Yu, N. J., Hubbell, W. L., and Hamm, H. E. (2002) Conformational Changes in the Amino-Terminal Helix of the G Protein α_{i1} Following Dissociation from G$\beta\gamma$ Subunit and Activation. *Biochemistry 41*, 9962–9972.
23. Preininger, A. M., Van Eps, N., Yu, N. J., Medkova, M., Hubbell, W. L., and Hamm, H. E. (2003) The Myristoylated Amino Terminus of Gα_{i1} Plays a Critical Role in the Structure and Function of Gα_{i1} Subunits in Solution. *Biochemistry 42*, 7931–7941.
24. Mumby, S. M., and Linder, M. E. (1994) Myristoylation of G-protein α subunits. *Methods Enzymol. 237*, 254–268.
25. Mazzoni, M. R., and Hamm, H. E. (1993) Tryptophan207 is involved in the GTP-dependent conformational switch in the α subunit of the G protein transducin: Chymotryptic digestion patterns of the GTPγS and GDP-bound forms. *J. Protein Chem. 12*, 215–221.
26. Mazzoni, M. R., Malinksi, J. A., and Hamm, H. E. (1991) Structural Analysis of Rod GTP-binding Protein, G_t. Limited Proteolytic Digestion Pattern of G_t with Four Proteases Defines Monoclonal Antibody Epitope. *J. Biol. Chem. 266*, 14072–14081.
27. Skiba, N. P., Bae, H., and Hamm, H. E. (1996) Mapping of Effector binding Sites of Transducin α-Subunit Using Gα_t/Gα_{i1} Chimeras. *J. Biol. Chem. 271*, 413–424.
28. Natochin, M., Granovsky, A. E., and Artemyev, N. O. (1998) Identification of effector residues on photoreceptor G protein, transducin. *J. Biol. Chem. 273*, 21808–21815.
29. Linder, M. E., Pang, I. H., Duronio, R. J., Gordon, J. I., Sternweis, P. C., and Gilman, A. G. (1991) Lipid Modifications of G Protein Subunits. Myristoylation of $G_{o\alpha}$ Increases its Affinity for $\beta\gamma$. *J. Biol. Chem. 266*, 4654–4659.
30. Imamoto, Y., Kataoka, M., Tokunaga, F., and Palczewski, K. (2000) Light-induced conformational changes of rhodopsin probed by fluorescent Alexa^{594} immobilized on the cytoplasmic surface. *Biochemistry 39*, 15225–15233.
31. Milligan, G. (2007) G protein-coupled receptor dimerisation: Molecular basis and relevance to function. *Biochim. Biophys. Acta 1768*, 825–835.
32. Liang, Y., Fotiadis, D., Filipek, S., Saperstein, D. A., Palczewski, K., and Engel, A. (2003) Organization of the G Protein-coupled Receptors Rhodopsin and Opsin in Native Membranes. *J. Biol. Chem. 278*, 21655–21662.
33. Cai, K., Itoh, Y., and Khorana, H. G. (2001) Mapping of contact sites in complex formation between transducin and light-activated rhodopsin by covalent crosslinking: Use of a photoactivatable reagent. *Proc. Natl. Acad. Sci. U.S.A. 98*, 4877–4882.
34. Marin, E. P., Krishna, A. G., Zvyaga, T. A., Isele, J., Siebert, F., and Sakmar, T. P. (2000) The Amino Terminus of the Fourth Cytoplasmic Loop of Rhodopsin Modulates Rhodopsin-Transducin Interaction. *J. Biol. Chem. 275*, 1930–1936.
35. Franke, R. R., Konig, B., Sakmar, T. P., Khorana, H. G., and Hofmann, K. P. (1990) Rhodopsin mutants that bind but fail to activate transducin. *Science 250*, 123–125.
36. Ernst, O. P., Meyer, C. K., Marin, E. P., Henklein, P., Fu, W. Y., Sakmar, T. P., and Hofmann, K. P. (2000) Mutation of the Fourth Cytoplasmic Loop of Rhodopsin Affects Binding of Transducin and Peptides Derived from the Carboxyl-terminal Sequences of Transducin α and γ Subunits. *J. Biol. Chem. 275*, 1937–1943.
37. Baneres, J. L., and Parello, J. (2003) Structure-based Analysis of GPCR Function: Evidence for a Novel Pentameric Assembly between the Dimeric Leukotriene B_4 Receptor BLT1 and the G-protein. *J. Mol. Biol. 329*, 815–829.
38. Blahos, J., Fischer, T., Brabet, I., Stauffer, D., Rovelli, G., Bockaert, J., and Pin, J. P. (2001) A novel site on the Gα-protein that recognizes heptahelical receptors. *J. Biol. Chem. 276*, 3262–3269.
39. Iiri, T., Farfel, Z., and Bourne, H. R. (1998) G-protein diseases furnish a model for the turn-on switch. *Nature 394*, 35–38.
40. Wall, M. A., Coleman, D. E., Lee, E., Iniguez-Lluhi, J. A., Posner, B. A., Gilman, A. G., and Sprang, S. R. (1995) The Structure of the G Protein Heterotrimer $G_{i\alpha1}\beta_1\gamma_2$. *Cell 83*, 1047–1058.
41. Pettersen, E. F., Goddard, T. D., Huang, C. C., Couch, G. S., Greenblatt, D. M., Meng, E. C., and Ferrin, T. E. (2004) UCSF Chimera: A visualization system for exploratory research and analysis. *J. Comput. Chem. 25*, 1605–1612.
42. Ramon, E., Marron, J., del Valle, L., Bosch, L., Andrews, A., Manyosa, J., and Garriga, P. (2003) Effect of dodecyl maltoside detergent on rhodopsin stability and function. *Vision Res. 43*, 3055–3061.
43. Whorton, M. R., Jastrzebska, B., Park, P. S. H., Fotiadis, D., Engle, A., Palczewski, K., and Sunahara, R. K. (2008) Efficient coupling of transducin to monomeric rhodopsin in a phospholipid bilayer. *J. Biol. Chem. 283*, 4387–4394.
44. Kahn, R. A., Randazzo, P., Serafini, T., Weiss, O., Rulka, C., Clark, J., Amherdt, M., Roller, P., Orci, L., and Rothman, J. E. (1992) The amino terminus of ADP-ribosylation factor (ARF) is a critical determinant of ARF activities and is a poetnt and specific inhibitor of protein transport. *J. Biol. Chem. 267*, 13039–13045.

BI800741R